

This article was downloaded by:[AMS/Barcelona Físic-Quim]  
[AMS/Barcelona Físic-Quim]

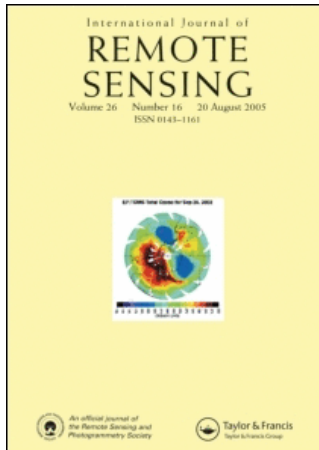
On: 3 February 2007

Access Details: [subscription number 731648980]

Publisher: Taylor & Francis

Informa Ltd Registered in England and Wales Registered Number: 1072954

Registered office: Mortimer House, 37-41 Mortimer Street, London W1T 3JH, UK



## International Journal of Remote Sensing

Publication details, including instructions for authors and subscription information:  
<http://www.informaworld.com/smpp/title-content=t713722504>

Comparison between Mallat's and the 'à trous' discrete wavelet transform based algorithms for the fusion of multispectral and panchromatic images

M. González-Audícana<sup>a</sup>; X. Otazu<sup>b</sup>; O. Fors<sup>c</sup>; A. Seco<sup>a</sup>

<sup>a</sup> Department of Projects and Rural Engineering, ETSIA, Public University of Navarre, Campus Arrosadía s/n. 31006 Pamplona. Spain

<sup>b</sup> Centre de Visió per Computador, Campus UAB, Edifici O, Cerdanyola del Vallès. 08193 Barcelona. Spain

<sup>c</sup> Department of Astronomy and Meteorology, University of Barcelona. C/Martí i Franquès 1, 08028 Barcelona. Spain

To link to this article: DOI: 10.1080/01431160512331314056

URL: <http://dx.doi.org/10.1080/01431160512331314056>

Full terms and conditions of use: <http://www.informaworld.com/terms-and-conditions-of-access.pdf>

This article maybe used for research, teaching and private study purposes. Any substantial or systematic reproduction, re-distribution, re-selling, loan or sub-licensing, systematic supply or distribution in any form to anyone is expressly forbidden.

The publisher does not give any warranty express or implied or make any representation that the contents will be complete or accurate or up to date. The accuracy of any instructions, formulae and drug doses should be independently verified with primary sources. The publisher shall not be liable for any loss, actions, claims, proceedings, demand or costs or damages whatsoever or howsoever caused arising directly or indirectly in connection with or arising out of the use of this material.

© Taylor and Francis 2007

## Comparison between Mallat's and the 'à trous' discrete wavelet transform based algorithms for the fusion of multispectral and panchromatic images

M. GONZÁLEZ-AUDÍCANA\*†, X. OTAZU‡, O. FORS§ and A. SECO†

†Department of Projects and Rural Engineering, ETSIA, Public University of Navarre, Campus Arrosadía s/n, 31006 Pamplona, Spain; e-mail: maria.audicana, and ros.secos@unavarra.es

‡Centre de Visió per Computador, Campus UAB, Edifici O, Cerdanyola del Vallès, 08193 Barcelona, Spain; e-mail: xotazu@cvc.uab.es

§Department of Astronomy and Meteorology, University of Barcelona, C/Martí i Franquès 1, 08028 Barcelona, Spain; e-mail: ofors@am.ub.es

(Received 17 February 2003; in final form 30 June 2004)

In the last few years, several researchers have proposed different procedures for the fusion of multispectral and panchromatic images based on the wavelet transform, which provide satisfactory high spatial resolution images keeping the spectral properties of the original multispectral data. The discrete approach of the wavelet transform can be performed with different algorithms, Mallat's and the 'à trous' being the most popular ones for image fusion purposes. Each algorithm has its particular mathematical properties and leads to different image decompositions. In this article, both algorithms are compared by the analysis of the spectral and spatial quality of the merged images which were obtained by applying several wavelet based, image fusion methods. All these have been used to merge Ikonos multispectral and panchromatic spatially degraded images. Comparison of the fused images is based on spectral and spatial characteristics and it is performed visually and quantitatively using statistical parameters and quantitative indexes.

In spite of its *a priori* lower theoretical mathematical suitability to extract detail in a multiresolution scheme, the 'à trous' algorithm has worked out better than Mallat's algorithm for image merging purposes.

### 1. Introduction

During the past few years, companies that distribute Earth observation satellite images have been offering mixed products with high spatial and spectral resolution. These are obtained by a combination of spatial information from panchromatic images and colour information from multispectral images, both acquired at the same time by sensors lodged at the same space platform. Two representative examples are the Ikonos and Quickbird pan-Sharpener images, offered by Space Imaging and Digital Globe, respectively. Given the design constraints of the sensors of these satellites, there is an inverse relation between their spectral and spatial resolution. Sensors with high spectral resolution, characterized by capturing the

---

\*Corresponding author.

radiance from different land covers in a high number of bands of the electromagnetic spectrum, do not show an optimal spatial resolution, and vice versa.

The availability of high spectral and spatial resolution images is important when undertaking studies in urban areas, heterogeneous forest areas or highly parcelled agricultural areas. On one hand, a high spectral resolution eases discrimination of land cover types. On the other hand, a high spatial resolution is necessary to be able to accurately delimit the area occupied by each land cover type, as well as to locate different terrain features and structures.

Fusion of multispectral and panchromatic images, with complementary spectral and spatial characteristics, is a widely used technique to obtain images with high spatial and spectral resolution simultaneously.

In the last few years, multiresolution analysis has become a suitable tool for the development of new image fusion methods. Recently, several researchers (Ranchin *et al.* 1993, 2003, Yocky 1995, Garguet-Duport *et al.* 1996, Couloigner *et al.* 1998, Zhou *et al.* 1998, Nuñez *et al.* 1999, Ranchin and Wald 2000, Aiazzi *et al.* 2002) have proposed different image fusion procedures using the multiresolution analysis based on the discrete wavelet transform (DWT), and proved that those methods provide an improved spatial resolution image, while keeping the spectral properties of the original multispectral data.

The discrete approach of the wavelet transform can be performed with several different approaches. Probably, the most popular ones for image fusion are Mallat's and the 'à trous' algorithms. Mallat's algorithm has been used, amongst others, by Ranchin *et al.* (1993), Yocky (1995), Garguet-Duport *et al.* (1996), Zhou *et al.* (1998) and Ranchin and Wald (2000), while the 'à trous' algorithm has been used by Nuñez *et al.* (1999), Chibani and Houacine (2002), González-Audiciana (2002) and Ranchin *et al.* (2003). Each one has its particular mathematical properties and leads to different image decompositions. The first is an orthogonal, dyadic, non-symmetric, decimated, non-redundant DWT algorithm. The 'à trous' is a non-orthogonal, shift-invariant, dyadic, symmetric, undecimated, redundant DWT algorithm. In this article, we compare both algorithms, analysing the spectral and spatial quality of the merged images that were obtained by applying several image fusion wavelet based methods.

All the fusion methods have been used to merge Ikonos multispectral with panchromatic images, corresponding to irrigated areas of Navarre, Spain. In order to assess the quality of the resulting images, these should be compared to the 'theoretical' images observed by the multispectral sensor if this would offer the same spatial resolution as the panchromatic one. As these images are not available we decided to work with spatially degraded images.

Comparison of the fused images is based on spectral and spatial characteristics and it is performed visually and quantitatively using statistical parameters (e.g. correlation coefficients, means difference) and quantitative indexes (e.g. Relative Average Spectral Error, RASE (Wald *et al.* 1997), Relative Adimensional Global Error of the Fusion, ERGAS (Wald 2000) or the Image Quality Index, Q (Wang and Bovik 2002)).

## 2. Multiresolution analysis and wavelet transform

Multiresolution analysis, based on wavelet theory, allows the decomposition of bidimensional datasets into different frequency components, and the study of each component with a resolution matched to its size. At a different resolution, the details of an image, i.e. high frequency components, characterize different physical features of the scene (Mallat 1989). At a coarse resolution, these details correspond to the

larger structures, while at a more detailed resolution, this information corresponds to the smaller size structures.

The wavelet transform provides a framework to decompose images into a number of new images, each of them with a decreasing degree of resolution, and to separate the spatial detail information of the image between two successive resolution degrees.

The continuous wavelet transform of a one-dimensional function,  $f(x) \in L^2(R)$ , with respect to the Mother Wavelet  $\psi(x)$  can be expressed as

$$W_f(a, b) = \langle f, \psi_{a,b} \rangle = \int_{-\infty}^{+\infty} f(x)\psi_{a,b}(x)dx \tag{1}$$

The wavelet base functions  $\psi_{a,b}(x)$  are dilations and translations of the Mother Wavelet  $\psi(x)$

$$\psi_{a,b}(x) = \frac{1}{\sqrt{a}}\psi\left(\frac{x-b}{a}\right) \tag{2}$$

where  $a, b \in R$ . Parameter ‘ $a$ ’ is the dilation or scaling factor, and parameter ‘ $b$ ’ is called the translation factor.

For every scale  $a$  and location  $b$ , the wavelet coefficient  $W_f(a, b)$  represents the information contained in  $f(x)$  at that scale and position.

The original signal can be exactly reconstructed from the wavelet coefficients by:

$$f(x) = \frac{1}{C_\psi} \int_0^\infty \int_{-\infty}^{+\infty} W_f(a,b)\psi_{a,b}(x)db \frac{da}{a^2} \tag{3}$$

where  $C_\psi$  is the normalizing factor of the Mother Wavelet.

The discrete approach of the wavelet transform can be carried out with several different algorithms.

### 2.1 Mallat’s algorithm

In order to understand the multiresolution analysis concept based on Mallat’s algorithm it is very useful to represent the wavelet transform as a pyramid, as shown in figure 1. The basis of the pyramid is the original image, with  $C$  columns and  $R$  rows. Each level of the pyramid, which is only accessible from the immediately lower level, is an approximation to the original image. When climbing up in the pyramid, the successive approximation images have a coarser spatial resolution. At the  $N$ th

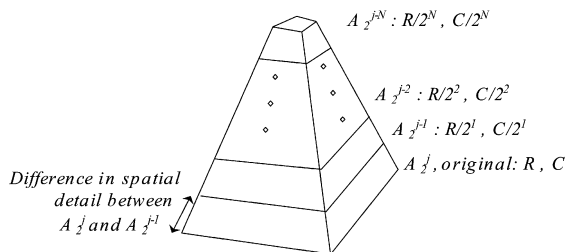


Figure 1. Pyramidal representation of Mallat’s wavelet decomposition algorithm.

level, the approximation image has  $C/2^N$  columns and  $R/2^N$  rows because a dyadic wavelet transform with subsampling or decimation is applied (Mallat 1989).

These approximation images are computed using scaling functions related to the Mother Wavelet function  $\psi(x)$  (Daubechies 1988, Mallat 1989). The difference between the information from two successive levels of the pyramid, e.g. between the original image  $A_2^j$  at a resolution  $2^j$  and the approximation image  $A_2^{j-1}$  at a resolution  $2^{j-1}$  is given by the wavelet transform, and computed using the wavelet functions. Three wavelet coefficient images,  $DH_2^{j-1}$ ,  $DV_2^{j-1}$  and  $DD_2^{j-1}$  pick up, respectively, the horizontal, vertical and diagonal detail that is lost between the images  $A_2^j$  and  $A_2^{j-1}$  and contain the features with sizes comprised between  $2^j$  and  $2^{j-1}$  resolution (non-redundant DWT algorithm). If the original image has  $C$  columns and  $R$  rows, the approximation and the wavelet coefficient images obtained applying this multiresolution decomposition have  $C/2$  columns and  $R/2$  rows.

When the inverse wavelet transform is applied, the original image  $A_2^j$  can be reconstructed exactly from the approximation image  $A_2^{j-1}$  and the horizontal, vertical and diagonal wavelet coefficients  $DH_2^{j-1}$ ,  $DV_2^{j-1}$  and  $DD_2^{j-1}$ .

For the practical implementation of Mallat's algorithm, quadrature mirror filters are used instead of the scaling and wavelet functions. The 'h' filter, associated with the scaling function, is a one-dimensional low pass filter that allows the analysis of low frequency data, while the 'g' filter, associated with the wavelet function, is a one-dimensional high pass filter that allows the analysis of the high frequency components, i.e. the detail of the image being analysed.

The number of parameters of these filters and the value of these parameters depend on the Mother Wavelet function used in this analysis. In this work, we have used the Daubechies four-coefficient wavelet basis. This leads to the following filters:

$$\begin{aligned} \mathbf{h} &: \left\{ \frac{(1-\sqrt{3})}{4\sqrt{2}}, \frac{(3-\sqrt{3})}{4\sqrt{2}}, \frac{(3+\sqrt{3})}{4\sqrt{2}}, \frac{(1+\sqrt{3})}{4\sqrt{2}} \right\} \\ \mathbf{g} &: \left\{ \frac{(1+\sqrt{3})}{4\sqrt{2}}, \frac{(3+\sqrt{3})}{4\sqrt{2}}, -\frac{(3-\sqrt{3})}{4\sqrt{2}}, \frac{(1-\sqrt{3})}{4\sqrt{2}} \right\} \end{aligned} \quad (4)$$

## 2.2 The 'à trous' algorithm

Another discrete approach of the wavelet transform is the 'à trous' algorithm (Holschneider and Tchamitchian 1990, Starck and Murtagh 1994). In this case, the image decomposition scheme cannot be represented with a pyramid as in Mallat's algorithm but with a parallelepiped. The basis of the parallelepiped is the original image,  $A_2^j$  at a resolution  $2^j$ , with  $C$  columns and  $R$  rows. Each level of the parallelepiped is an approximation to the original image, as in Mallat's algorithm. When climbing up through the resolution levels, the successive approximation images have a coarser spatial resolution but the same number of pixels as the original image, as shown in figure 2. If a dyadic decomposition approach is applied, the resolution of the approximation image at the  $N$ th level is  $2^{j-N}$ .

These approximation images are computed using scaling functions. The spatial detail that is lost between the images  $A_2^{j-1}$  and  $A_2^j$  is collected in just one wavelet

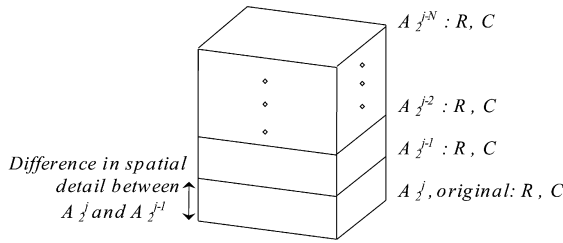


Figure 2. Parallelepiped representation of the ‘à trous’ wavelet decomposition algorithm.

coefficient image,  $w_2^{j-1}$ , frequently called wavelet plane. This wavelet plane, which globally represents the horizontal, vertical and diagonal spatial detail between  $2^j$  and  $2^{j-1}$  resolution, is computed as the difference between  $A_2^{j-1}$  and  $A_2^j$ , i.e. two consecutive levels of the parallelepiped. When the inverse transform is applied, the original image  $A_2^j$  can be reconstructed exactly adding to the approximation image  $A_2^{j-1}$  the wavelet plane  $w_2^{j-1}$ .

In contrast to Mallat’s algorithm, the ‘à trous’ algorithm allows a shift-invariant discrete wavelet decomposition. All the approximation images obtained by applying this decomposition have the same number of columns and rows as the original image. This is a consequence of the fact that the ‘à trous’ algorithm is a non-orthogonal, redundant oversampled transform (Vetterli and Kovacevic 1995).

For the practical implementation of the ‘à trous’ algorithm, a two-dimensional filter associated to the scaling function is used. In this work, we use a scaling function that has a  $B_3$  cubic spline profile. This function leads to the following low pass filter:

$$\frac{1}{256} \begin{pmatrix} 1/256 & 1/64 & 3/128 & 1/64 & 1/256 \\ 1/64 & 1/16 & 3/32 & 1/16 & 1/64 \\ 3/128 & 3/32 & 9/64 & 3/32 & 3/128 \\ 1/64 & 1/16 & 3/32 & 1/16 & 1/64 \\ 1/256 & 1/64 & 3/128 & 1/64 & 1/256 \end{pmatrix} \quad (5)$$

As we filter to obtain coarser approximations of the original image, the above filter must be filled with zeros, in order to match the resolution of desired level.

As mentioned previously, and contrary to Mallat’s algorithm, the ‘à trous’ algorithm is non-orthogonal and this implies that the wavelet plane  $w_2^{j-1}$  for a given scale  $2^{j-1}$  could retain information for the neighbouring scale  $2^j$ .

### 3. Image fusion methods based on the DWT

The central idea of all image fusion methods based on multiresolution analysis and the DWT is to extract from the panchromatic image the spatial detail that is not present in the multispectral image in order to insert it later in the latter. The detailed information of the panchromatic image that corresponds to structures or features with a size between the spatial resolution of the panchromatic image and that of the multispectral one can be extracted using Mallat’s or the ‘à trous’ DWT algorithms. Such information is collected in the wavelet coefficient images or wavelet planes and it could be directly injected into the multispectral image without modifying its total flux because these wavelet coefficient images have zero mean.

According to the procedures used to insert or inject the spatial detail of the panchromatic image into the multispectral image, is possible to distinguish at least three different image fusion methods based on the DWT:

- (a) Additive Wavelet method;
- (b) Additive Wavelet Intensity method;
- (c) Additive Wavelet Principal Component method

In addition, substitutive image fusion methods based on the DWT can be found in recent literature (e.g. Yocky 1995, Gauguet-Duport *et al.* 1996, Zhou *et al.* 1998, Ranchin and Wald 2000).

When Mallat's algorithm is used to perform the wavelet decomposition, the quality of the merged images obtained via substitutive approaches is similar to that of the merged images obtained via additive approaches. However, when the 'à trous' algorithm is used, the additive approaches offer significantly better performance than the substitutive ones (Nuñez *et al.* 1999, González-Audícana *et al.* 2002). If we want to compare Mallat's algorithm and the 'à trous' algorithm, the implementation schemes have to be equivalent. This is why we decided to work in both cases with additive approaches.

In order to apply any of the image fusion methods described in this section, it is necessary that the multispectral and the panchromatic images can be accurately superimposed. Therefore, both images have to be co-registered and the multispectral image needs to be resampled to make its pixel size the same as the panchromatic one.

### 3.1 Additive Wavelet method (AW)

In this case, discrete wavelet transforms are used to extract, from the panchromatic image, just the spatial detail information missing in the multispectral image, to insert later into each band of the multispectral image. Both the extraction and injection of spatial detail can be done using Mallat's or the 'à trous' wavelet decomposition algorithms.

**3.1.1 Additive Wavelet method using Mallat's algorithm.** The steps for merging Ikonos multispectral and panchromatic images using this method are as follows.

- (1) Generate new panchromatic images, whose histograms match those of each band of the multispectral image.
- (2) Apply the wavelet transform to the 'histogram-matched' panchromatic images. As the spatial resolution ratio between the panchromatic and multispectral Ikonos images is 4:1, it is necessary to perform a second level wavelet transform. Repeat the same transform to each multispectral band, using the Daubechies four-coefficient wavelet basis. From each multispectral and panchromatic wavelet image decomposition, seven quarter-resolution images are obtained. The first one is a low frequency version of the original image, and the other six images, the wavelet coefficient images.
- (3) Introduce the detail of the panchromatic image into each multispectral band adding the wavelet coefficients of the panchromatic image to those of the multispectral image and later applying the inverse wavelet transform.

This image fusion method has been used in a substitutive way by Ranchin *et al.* (1993), Yocky (1995), Gauguet-Duport *et al.* (1996), Wald *et al.* (1997), Zhou *et al.* (1998) and Ranchin and Wald (2000), amongst others.

**3.1.2 Additive Wavelet method using the ‘à trous’ algorithm.** The steps for merging Ikonos multispectral and panchromatic images using this method are as follows.

- (1) Generate new panchromatic images, whose histograms match those of each band of the multispectral image.
- (2) Perform the second level wavelet transform only on the panchromatic images.
- (3) Add the wavelet planes of the panchromatic decomposition to each band of the multispectral dataset.

This image fusion method has been firstly used by Nuñez *et al.* (1999).

### 3.2 Additive Wavelet Intensity method (AWI)

Probably the most popular method used to merge multispectral and panchromatic images is the Component Substitution method based on the Intensity–Hue–Saturation (IHS) transformation (Haydn *et al.* 1982). The widespread use of this procedure to merge images relies on the fact that IHS transform can take apart the colour information of an RGB composition in its components Hue and Saturation and isolate in the Intensity component most of the spatial information (Pohl and Van Genderen 1998).

In contrast to the standard IHS merger, the basic idea of the AWI method is to insert the spatial detail of the panchromatic image into the intensity component of the multispectral image that gathers most of its spatial information, instead of replacing this component with the whole panchromatic image.

Several algorithms have been developed for converting colour RGB values into values of IHS. These differ not only in their processing time, but also in the methodology used to calculate the value of the Intensity. We chose the algorithm based on Smith’s triangle model (Smith 1978), which considers the Intensity as the average of the three RGB values, because this was the one that offered the best relative results when applied to image fusion (Nuñez *et al.* 1999, González-Audicana *et al.* 2002).

**3.2.1 Additive Wavelet Intensity method using Mallat’s algorithm.** The steps for merging Ikonos images using this method are the following.

- (1) Apply the IHS transform to the RGB composition of the multispectral image. This transformation separates the spatial information of the multispectral image into the Intensity component.
- (2) Generate a new panchromatic image, whose histogram matches the histogram of the Intensity image.
- (3) Apply Mallat’s decomposition algorithm to the Intensity image and to the ‘histogram-matched’ panchromatic one. Both second level decompositions are computed using the Daubechies four-coefficient wavelet basis. Extract the wavelet coefficients that pick up the horizontal, vertical and diagonal

spatial detail present in the panchromatic image and missing in the multispectral image.

- (4) Add this spatial detail information into the Intensity image applying the inverse wavelet transform to the set composed by the Intensity approximation image and the sum of the wavelet coefficients of the initial Intensity and panchromatic images.
- (5) Insert the spatial information of the panchromatic image into the multispectral one, applying the inverse IHS transform.

Figure 3 shows how this method has been applied to fuse Ikonos multispectral and panchromatic spatially degraded images (with a spatial resolution of 4 m and 16 m, respectively). This image fusion alternative was applied by González-Audicana (2002) and González-Audicana *et al.* 2002.

**3.2.2 Additive Wavelet Intensity method using the ‘à trous’ algorithm.** This method was defined by Nuñez *et al.* (1999). The steps for merging Ikonos multispectral and panchromatic images using this method are:

- (1) Apply the IHS transform to the RGB composition of the multispectral image and obtain the Intensity component.
- (2) Generate a new panchromatic image, whose histogram matches the histogram of the Intensity image.
- (3) Decompose only the ‘histogram-matched’ panchromatic image, using the ‘à trous’ DWT algorithm, and obtain the first and second wavelet planes that pick up the high frequency elements, i.e. the spatial detail of this image not present in the multispectral one.

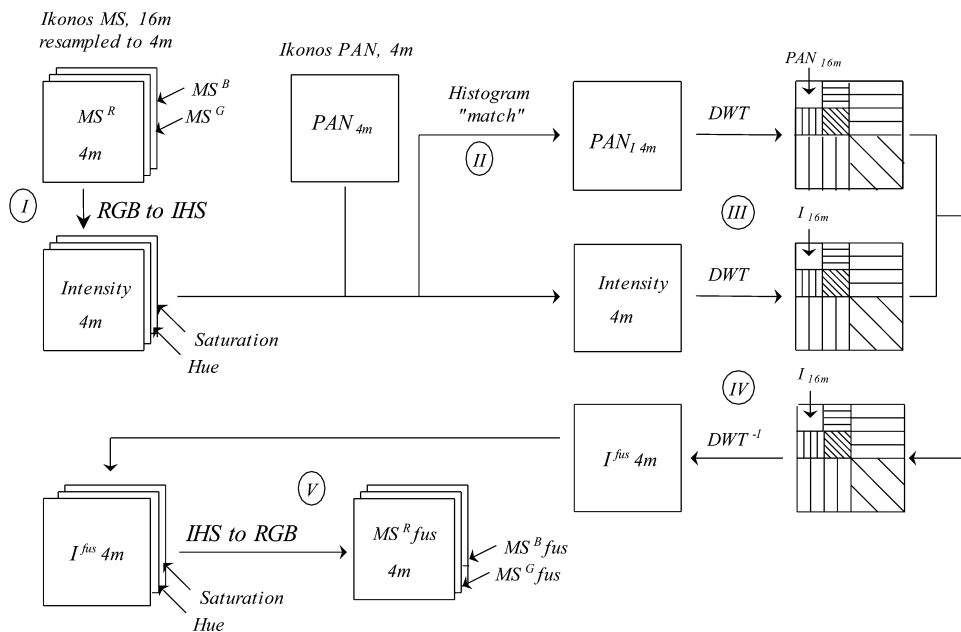


Figure 3. Fusion of Ikonos spatially degraded images applying the AWI method using Mallat's algorithm.

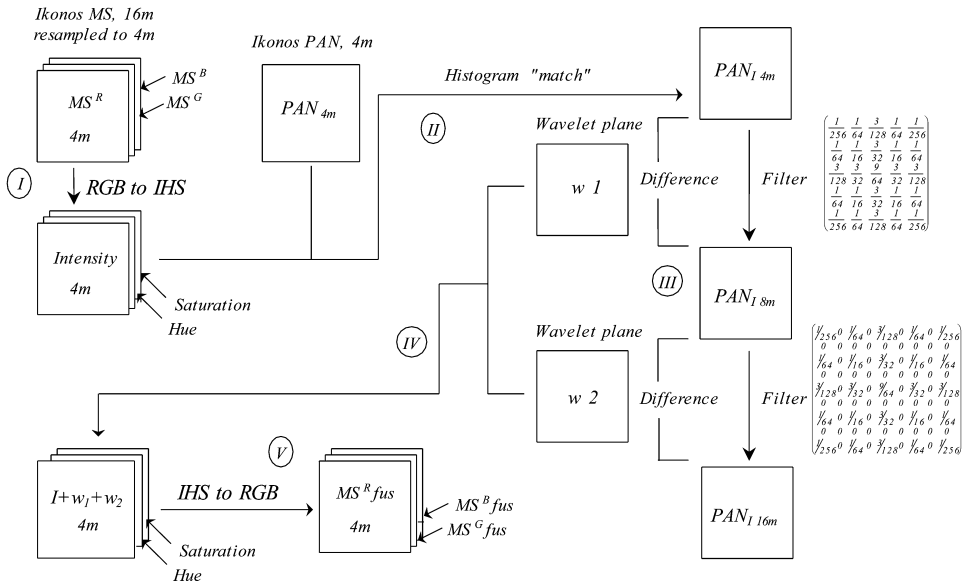


Figure 4. Fusion of Ikonos spatially degraded images applying the AWI method using the ‘à trous’ algorithm.

- (4) Add these wavelet planes to the I image, as shown in figure 4.
- (5) Insert the spatial information of the panchromatic image into the multispectral one through the inverse IHS transform.

One of the disadvantages of the fusion methods based on the IHS transform is that they can only be applied to three-band RGB compositions. In this case, and in order to compare these methods with other fusion methods, all the algorithms described before were repeated for the four possible RGB compositions of the initial Ikonos multispectral image. This implies that for each spectral band we obtain three merged bands coming from the different RGB compositions. The final merged image is formed by the triplet of merged bands that have the highest spectral correlation with the respective spectral bands of the original Ikonos multispectral image.

### 3.3 Additive Wavelet Principal Component method (AWPC)

Another classical component substitution method (Shettigara 1992) widely used to merge multispectral and panchromatic images, is that based on Principal Component Analysis (PCA). As in the IHS transform, PCA isolates the spatial information in the first principal component assuming that the original multispectral image covers mainly vegetated areas (Chavez and Kwarteng 1989). When the standard PCA merger is applied, the whole panchromatic image replaces the first principal component and its spatial and also its spectral information is inserted into the multispectral one through the inverse PCA. In contrast, when the AWPC method is used, just the spatial detail of the panchromatic image missing in the multispectral one is added to the first principal component and finally inserted into the multispectral one through the inverse PCA transformation.

We can distinguish two methodological alternatives of the AWPC, according to the algorithm used to extract the spatial detail of the panchromatic image: the AWPC Mallat's method and the AWPC 'à trous' method. In any case, the procedure used to merge images using AWPC methods is similar to that of the AWI methods, applying the PCA instead of the IHS transformation and adding the spatial detail of the panchromatic image to the first principal component instead of to the Intensity component.

The AWPC method using the Mallat's and the 'à trous' algorithm was applied by González-Audícana *et al.* 2002.

#### 4. Results

The AW, AWI and AWPC methods, applying both Mallat's and 'à trous' algorithms have been used to merge Ikonos multispectral and panchromatic images. These images, acquired in October 2000, cover the agricultural irrigated area of Mendavia (Navarre), in northern Spain. Corn, alfalfa and grapes were the main crops in 2000.

##### 4.1 Spatial degradation

As is well known, the spatial resolution of the Ikonos multispectral and panchromatic images is 4 m and 1 m, respectively. The high spatial resolution multispectral images obtained applying any of the image fusion methods would have an actual spatial resolution similar to that of the panchromatic image. In order to assess the quality of the merged images using Mallat's or the 'à trous' algorithm, they should be compared with the 'theoretical' image observed by the multispectral sensor if this offered the same spatial resolution as the panchromatic one. Since these images do not exist, we worked with spatially degraded images. Thus, the Ikonos multispectral and panchromatic images were degraded to 16 m and 4 m, respectively.

Merged images obtained by different fusion methods have a spatial resolution of 4 m, so the accuracy of each image fusion method can be evaluated by comparing the resulting merged images with the Ikonos multispectral original one. The comparison between the original and the different merged images is based on spectral and spatial criteria, and is done both visually and quantitatively.

##### 4.2 Spectral quality of the merged images

In order to be able to use the merged images to extract thematic information such as agricultural crop distribution, change detection or land uses mapping through a multispectral classification, it is necessary that the image fusion process does not modify the spectral information of the initial multispectral image.

Ikonos merged images obtained by applying any of the fusion methods described before have a spatial resolution of 4 m so their spectral quality can be evaluated by comparing its spectral information to that of the Ikonos original multispectral image.

The spectral quality assessment procedure is based on visual inspection and the use of the following quantitative indicators.

- (i) Correlation coefficient between the original and the merged images. It should be as close to 1 as possible.

- (ii) Difference between the means of the original and the merged images, in radiance. It should be as close as possible to 0.
- (iii) Standard deviation of the difference image, in radiance. It globally indicates the level of error at any given pixel (Wald *et al.* 1997). The lower the value of this parameter, the better the spectral quality of the merged image.

These parameters allow us to determine the difference in spectral information between each band of the merged image and of the original image.

In order to estimate the global spectral quality of the merged images, we have used the following parameters.

- (a) The ERGAS index (Erreur Relative Globale Adimensionnelle de Synthèse) or relative dimensionless global error in the fusion (Wald 2000):

$$\text{ERGAS} = 100 \frac{h}{l} \sqrt{\frac{1}{N} \sum_{i=1}^n \left( \text{RMSE}^2(B_i) / M_i^2 \right)} \quad (6)$$

where  $h$  is the resolution of the panchromatic image,  $l$  the resolution of the multispectral image,  $N$  the number of spectral bands ( $B_i$ ) involved in the fusion,  $M_i$  the mean radiance of each spectral band and RMSE the root mean square error computed

$$\text{RMSE}^2(B_i) = \text{mean difference}^2(B_i) + \text{standard deviation}^2(B_i) \quad (7)$$

The lower the ERGAS value the higher the spectral quality of the merged images.

- (b) The Image Quality Index, Q, proposed by Wang and Bovik (2002):

$$Q = \frac{4\sigma_{OF}\bar{O}\bar{F}}{(\sigma_O^2 + \sigma_F^2) \left[ (\bar{O})^2 + (\bar{F})^2 \right]} \quad (8)$$

where  $\bar{O}$  and  $\bar{F}$  are the mean of each original ( $O$ ) and fused ( $F$ ) images,  $\sigma_O^2$  and  $\sigma_F^2$  the variances of  $O$  and  $F$  and  $\sigma_{OF}$  the covariance between  $O$  and  $F$ . The Q index models the difference between two images as a combination of three different factors: loss of correlation, luminance distortion and contrast distortion. As image quality is often space dependent, Wang and Bovik recommend to calculate the Q index using a sliding window approach. In this work, sliding windows with a size of  $8 \times 8$ ,  $16 \times 16$ ,  $32 \times 32$ ,  $64 \times 64$  and  $128 \times 128$  pixels are used. As the Q index can only be applied to monochromatic images, the average value ( $Q_{\text{avg}}$ ) is used as a quality index for multispectral images. The higher the  $Q_{\text{avg}}$  value the higher the spectral and radiometric quality of the merged images.

Table 1 shows the results obtained for the indexes described above when the Ikonos merged images (4 m per pixel) were compared to the Ikonos original multispectral image (4 m per pixel).

In order to quantify the actual effect that fusion has on the initial multispectral image (spatially degraded image), we show in the first column the values of the different parameters obtained when this degraded image is compared with the original multispectral image. Therefore, this first column reflects the situation before

Table 1. Value of the different parameters analysed to estimate the spectral quality of the merged images.

		X degraded	AW 'à trous'	AW Mallat	AWI 'à trous'	AWI Mallat	AWPC 'à trous'	AWPC Mallat	Ideal
Spectral correlation coefficient	X1	0.9116	0.9491	0.9405	0.9374	0.9289	0.9517	0.9443	1
	X2	0.9014	0.9558	0.9455	0.9601	0.9518	0.9568	0.9475	1
	X3	0.9126	0.9577	0.9485	0.9668	0.9601	0.9592	0.9510	1
	X4	0.8572	0.9291	0.9157	0.9307	0.9188	0.9249	0.9167	1
Mean difference (BIAS)	X1	0.0224	0.0225	0.0146	0.0386	0.0483	0.0225	0.0203	0
	X2	0.0210	0.0209	0.0131	0.0226	0.0140	0.0208	0.0172	0
	X3	0.0158	0.0155	0.0095	0.0005	0.0048	0.0155	0.0119	0
	X4	0.0186	0.0170	0.0102	0.0769	0.0716	0.0169	0.0149	0
Standard deviation of the difference image	X1	0.2503	0.2164	0.2254	0.2529	0.2537	0.2082	0.2180	0
	X2	0.4437	0.3418	0.3647	0.3108	0.3362	0.3357	0.3597	0
	X3	0.4062	0.3358	0.3546	0.2776	0.3034	0.3269	0.3475	0
	X4	0.5278	0.4656	0.4949	0.4480	0.4814	0.4654	0.4938	0
ERGAS		1.81	1.91	1.70	1.81	1.72	1.88	0	
Q <sub>avg</sub> 8 × 8		0.500	0.745	0.698	0.746	0.701	0.744	0.699	1
Q <sub>avg</sub> 16 × 16		0.667	0.835	0.804	0.838	0.808	0.837	0.806	1
Q <sub>avg</sub> 32 × 32		0.761	0.886	0.864	0.888	0.867	0.888	0.866	1
Q <sub>avg</sub> 64 × 64		0.815	0.915	0.898	0.915	0.899	0.917	0.901	1
Q <sub>avg</sub> 128 × 128		0.843	0.930	0.916	0.930	0.917	0.931	0.919	1

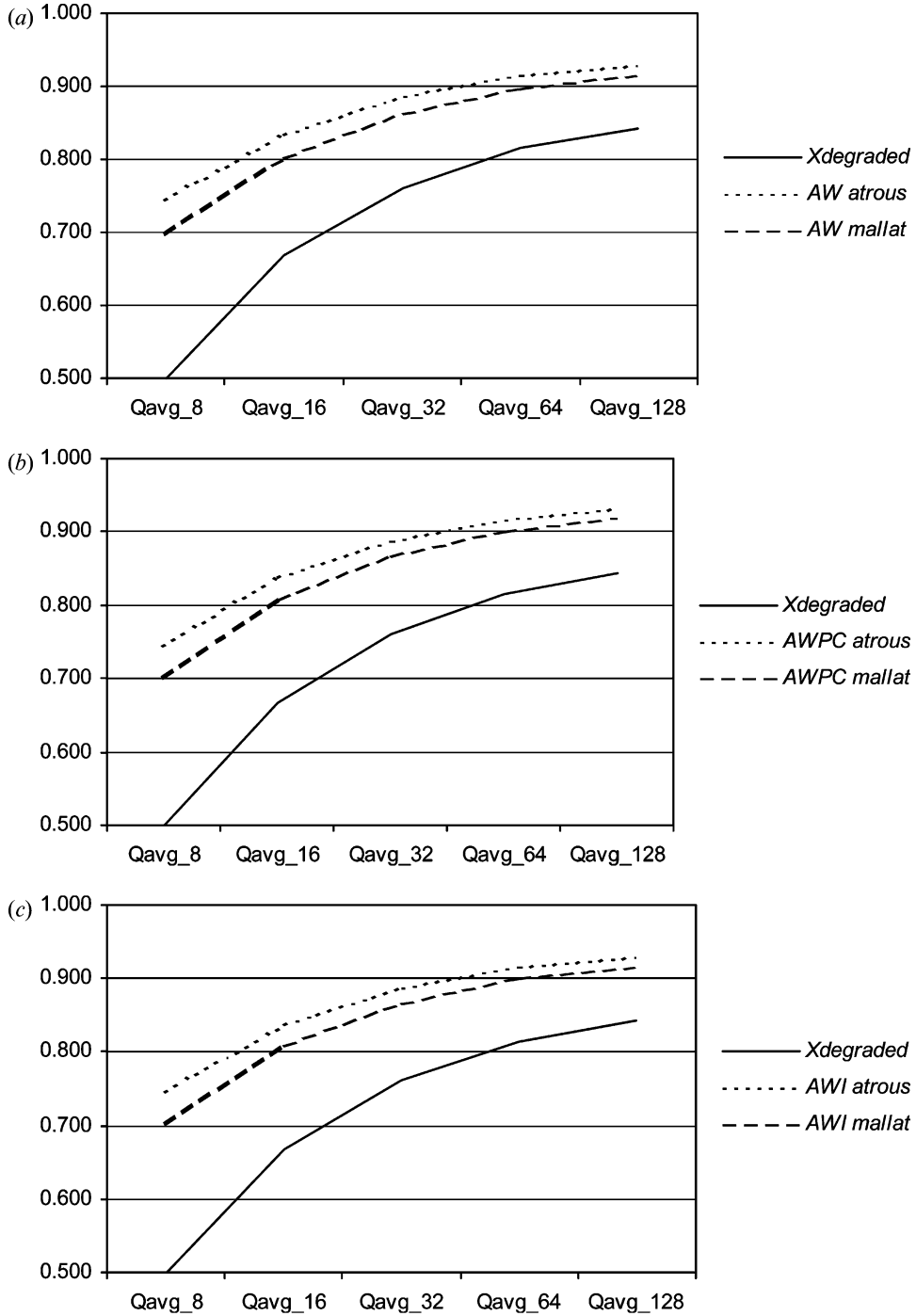


Figure 5. Graphical representation of the  $Q_{avg}$  values of the Ikonos merged images for different sliding windows sizes.

the fusion, while the last column reflects the situation that ideally should be reached after the fusion.

Lower ERGAS and higher  $Q_{avg}$  values than those shown in the first column indicate that the fusion method yields to a merged image closer to that collected by the multispectral sensor if it had the same spatial resolution as the panchromatic.

To ease the comparison of the different fusion methods according to the  $Q_{avg}$  parameter, we have displayed the  $Q_{avg}$  values for different sliding sizes windows in figure 5.

As mentioned in section 2.2, the ‘à trous’ algorithm, contrary to Mallat’s algorithm, is non-orthogonal, which implies that a wavelet plane of the panchromatic image could retain information for a neighbouring plane. It could be thought that this non-orthogonality might have a negative influence on the spectral quality of the merged images. On the contrary, the AW, AWI and AWPC methods based on the ‘à trous’ algorithm have led to images with slightly better spectral quality than the corresponding methods based on Mallat’s algorithm. The ERGAS values obtained with the former are lower than those obtained with the latter. Spectrally, the AWI method using the ‘à trous’ algorithm leads to the highest quality image, i.e. the image with spectral information very similar to that of the Ikonos original multispectral image.

### 4.3 Spatial quality of the merged images

A high spatial quality merged image is that which incorporates the spatial detail features present in the panchromatic image and missing in the initial multispectral one. To assess the spatial quality of any merged image, its spatial detail information must be compared to the that present in the panchromatic image. This comparison was performed both visually and quantitatively. Just a couple of quantitative procedures have been found in current literature to evaluate the spatial quality of merged images: the procedure proposed by Zhou *et al.* (1998) based on the correlation coefficient estimation between high-pass filtered images, and that proposed by Li (2000), based on the blur parameter estimation.

To evaluate the spatial quality of the Ikonos merged images, we used the procedure proposed by Zhou *et al.* (1998). This procedure is based on the fact that the spatial information of an image is mostly concentrated in the high frequency domain. Comparing the high frequency information of the merged images with that of the reference image it will be possible to assess quantitatively the spatial quality of a merged image. In order to extract the spatial detail of the images to be compared, these are high pass filtered. We have used the following Laplacian filter:

$$\begin{bmatrix} -1 & -1 & -1 \\ -1 & 8 & -1 \\ -1 & -1 & -1 \end{bmatrix} \quad (8)$$

The correlation coefficient as well as the  $Q_{avg}$  index values between the high-pass filtered merged image and the high-pass filtered reference image can be considered as an index of the spatial quality of the merged image.

If the Ikonos panchromatic initial image is used as reference and its spatial detail information compared to that of the multispectral original and merged images, it

will be possible to calculate how much detailed information has been incorporated into the latter during the fusion process. Therefore, the panchromatic initial image, the merged images and the initial multispectral image were filtered using the Laplacian filter described above. The  $Q_{avg}$  index was calculated for different sliding window sizes and these values, together with the correlation coefficients, are shown in table 2.

The first column shows the spatial correlation coefficients and the  $Q_{avg}$  values between the panchromatic and the multispectral initial images (degraded images) and reflects the situation before the fusion, while the last one reflects what would be the ideal ending situation, from the spatial quality point of view, when the fusion process is completed.

The high spatial correlation and  $Q_{avg}$  values shown in table 2 for the different merged images indicate that the main part of the spatial information from the panchromatic image has been incorporated during the fusion process. This spatial detail incorporation is slightly higher in those merged images obtained using the 'à trous' algorithm than in those obtained using Mallat's algorithm (figure 6).

This spatial quality difference between the 'à trous' and Mallat's merged images can also be detected when colour compositions are visually compared. If the colour compositions of the merged images obtained using Mallat's algorithm (figures 7(d), (f) and (h)) are analysed and compared to that of the Ikonos original multispectral image (figure 7(a)), artefacts in structures with neither horizontal nor vertical direction are detected. In these images, the field roads and irrigation ditches oriented in the horizontal and vertical directions preserve their linear continuity. However, this linear continuity has been reduced in those field roads and ditches oriented in other directions, showing up a discontinuity or noise effect along their path.

When Mallat's algorithm is used to perform the discrete wavelet decomposition of an image, a subsampling or decimation process is applied. This decimation process applied separately to the rows and columns of the image to be decomposed, causes a loss of linear continuity in those spatial features with neither horizontal nor vertical directions. Mallat's decimated algorithm is less suitable for extracting orientation-independent detail from an image than the 'à trous' undecimated algorithm, which preserves the features path continuity.

The higher suitability of the 'à trous' algorithm to extract rotation-invariant feature edges is shown when the composition of the 'à trous' merged images are compared to those of Mallat's merged images, as well as to that of the multispectral original image (figure 7).

## 5. Conclusions

In this article, Mallat's and the 'à trous' DWT based fusion approaches have been compared. Their suitability to merge Ikonos images has been evaluated by means of spectral and spatial analysis.

The global quality assessment of all merged images has demonstrated that both algorithms allow the extraction of spatial information from the panchromatic image missing in the multispectral image. This is inserted into the multispectral image without modifying its spectral information content.

Different image fusion methods based on the 'à trous' and Mallat's algorithm (AW, AWI and AWPC) have been compared. The non-orthogonality of the 'à trous' algorithm might have a negative influence on the spectral quality of the

Table 2. Value of the spatial correlation coefficient and  $Q_{\text{avg}}$  values between the panchromatic and different merged filtered images.

		$X_{\text{degraded}}$	AW 'à trous'	AW Mallat	AWI 'à trous'	AWI Mallat	AWPC 'à trous'	AWPC Mallat	Ideal
Spatial correlation coefficient	X1	0.179	0.975	0.920	0.977	0.920	0.956	0.926	1
	X2	0.195	0.975	0.922	0.961	0.912	0.958	0.928	1
	X3	0.193	0.978	0.924	0.947	0.901	0.960	0.930	1
	X4	0.204	0.965	0.917	0.949	0.903	0.917	0.897	1
$Q_{\text{avg}} 8 \times 8$		0.073	0.916	0.849	0.912	0.851	0.875	0.840	1
$Q_{\text{avg}} 16 \times 16$		0.089	0.926	0.871	0.926	0.874	0.9023	0.861	1
$Q_{\text{avg}} 32 \times 32$		0.0914	0.931	0.884	0.933	0.885	0.921	0.868	1
$Q_{\text{avg}} 64 \times 64$		0.0878	0.933	0.886	0.936	0.891	0.918	0.875	1
$Q_{\text{avg}} 128 \times 128$		0.086	0.934	0.889	0.938	0.895	0.920	0.878	1

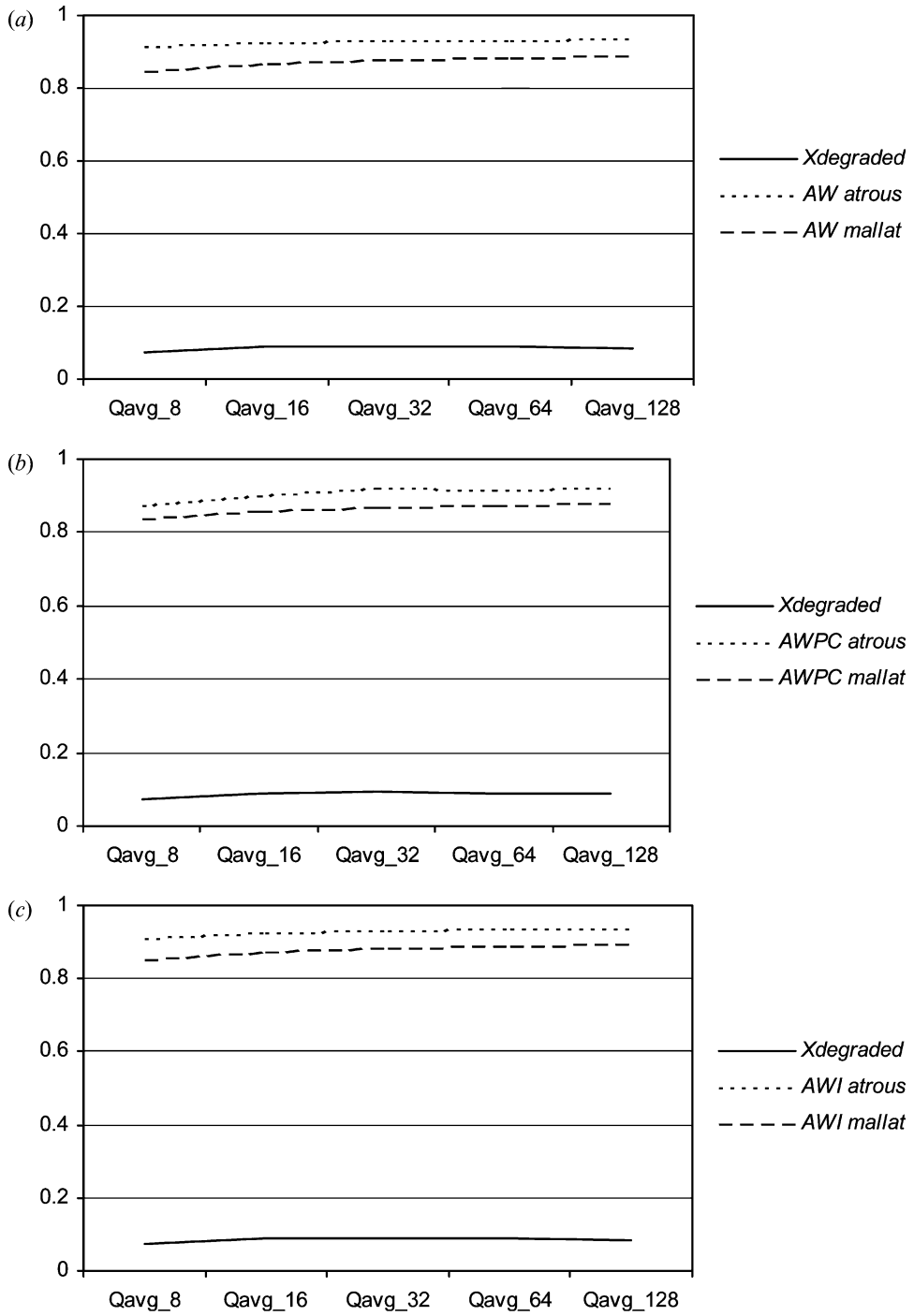


Figure 6. Graphical representation of the  $Q_{avg}$  values of the Ikonos merged images for different sliding windows sizes when compared to the Ikonos panchromatic image.

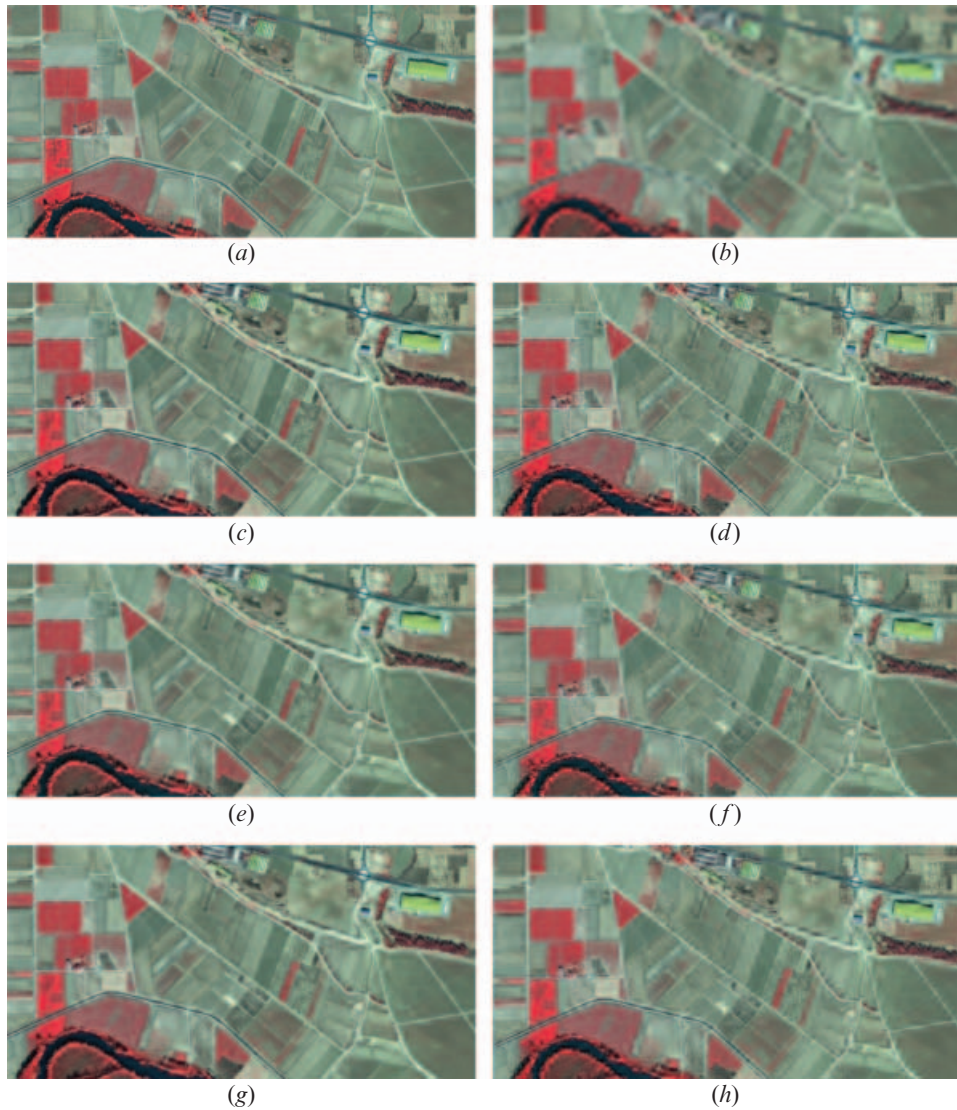


Figure 7. False colour composition of part of the Ikonos images. (a) Multispectral original image; (b) multispectral initial image, spatially degraded image; (c) AW ‘à trous’ merged image; (d) AW Mallat merged image; (e) AWI ‘à trous’ merged image; (f) AWI Mallat merged image; (g) AWPC ‘à trous’ merged image; (h) AWPC Mallat merged image.

merged images. However, the ERGAS value as well as the  $Q_{avg}$  for all the merged images obtained using this DWT algorithm are slightly better than those obtained by Mallat’s orthogonal algorithm. Spectrally, the ‘à trous’ algorithm works out as well as the Mallat’s algorithm for image merging purpose.

Due to the decimation process of Mallat’s algorithm strongly oriented in the horizontal and vertical directions, the resulting merged images present, visually, a lower spatial quality than those obtained using the ‘à trous’ algorithm.

## References

- AIAZZI, B., ALPARONE, L., BARONTI, S. and GARZELLI, A., 2002, Context-driven fusion of high spatial and spectral resolution images based on oversampled multiresolution analysis. *IEEE Transactions on Geoscience and Remote Sensing*, **40**, pp. 2300–2312.
- CHAVEZ, P.S. and KWARTENG, A.Y., 1989, Extracting spectral contrast in Landsat Thematic Mapper image data using selective principal component analysis. *Photogrammetric Engineering and Remote Sensing*, **55**, pp. 339–348.
- CHIBANI, Y. and HOUACINE, A., 2002, The joint use of IHS transform and redundant wavelet decomposition for fusing multispectral and panchromatic images. *International Journal of Remote Sensing*, **23**, pp. 3821–3833.
- COULOIGNER, I., RANCHIN, T., VALTONEN, V.P. and WALD, L., 1998, Benefit of the future SPOT-5 and of data fusion to urban roads mapping. *International Journal of Remote Sensing*, **19**, pp. 1519–1532.
- DAUBECHIES, I., 1988, Orthonormal basis of compactly supported wavelets. *Communications on Pure Applied Mathematics*, **41**, pp. 909–996.
- GARGUET-DUPORT, B., GIREL, J., CHASSENY, J.M. and PAUTOU, G., 1996, The use of multiresolution analysis and wavelets transform for merging SPOT panchromatic and multispectral image data. *Photogrammetric Engineering and Remote Sensing*, **62**, pp. 1057–1066.
- GONZÁLEZ-AUDÍCANA, M., 2002, Fusión de imágenes multiespectrales y pancromáticas: desarrollo, aplicación y comparación de diferentes procedimientos. Utilidad de las imágenes resultantes para la discriminación de cultivos en áreas de regadío de Navarra. Eng. Doctoral Thesis, Universidad Pública de Navarra, Spain.
- GONZÁLEZ-AUDÍCANA, M., OTAZU, X., FORS, O., GARCIA, R. and NUÑEZ, J., 2002, Fusion of different spatial and spectral resolution images: development, application and comparison of new methods based on wavelets. *Proceedings of the International Symposium on Recent Advances in Quantitative Remote Sensing*, 16–20 September 2002, Valencia, pp. 228–237.
- HAYDN, R., DALKE, G.W., HENKEL, J. and BARE, J.E., 1982, Applications of the IHS color transform to the processing of multisensor data and image enhancement. *Proceedings of the International Symposium on Remote Sensing of Arid and Semi-Arid Lands, January* (Cairo: ISRS), pp. 559–616.
- HOLSCHNEIDER, M. and TCHAMITCHIAN, P., 1990, Régularité locale de la fonction ‘non-differentiable’ the Riemann. In *Les Ondelettes en 1989*, P.G. Lemarié (Ed.) (Paris: Springer-Verlag), pp. 102–124.
- LI, J., 2000, Spatial quality evaluation of fusion of different resolution images. *Proceedings of the 19th ISPRS Congress, July 2000, Amsterdam* (Amsterdam: IAPRS), Vol. XXXIII.
- MALLAT, S.G., 1989, A theory for multiresolution signal decomposition: the wavelet representation. *IEEE Transactions on Pattern Analysis and Machine Intelligence*, **11**, pp. 674–693.
- NUÑEZ, J., OTAZU, X., FORS, O., PRADES, A., PALA, V. and ARBIOL, R., 1999, Multiresolution-based image fusion with additive wavelet decomposition. *IEEE Transactions on Geoscience and Remote Sensing*, **37**, pp. 1204–1211.
- POHL, C. and VAN GENDEREN J.L., 1998, Multisensor image fusion in remote sensing: concepts, methods and applications. *International Journal of Remote Sensing*, **19**, pp. 823–854.
- RANCHIN, T. and WALD, L., 2000, Fusion of high spatial and spectral resolution images: the ARSIS concept and its implementation. *Photogrammetric Engineering and Remote Sensing*, **66**, pp. 49–61.
- RANCHIN, T., WALD, L. and MANGOLINI, M., 1993, Efficient data fusion using wavelet transform: the case of SPOT satellite images. *Proceedings of the International Symposium on Optics, Imaging and Instrumentation*, A.F. Laivre (Ed.) (San Diego, CA: SPIE), pp. 171–178.

- RANCHIN, T., AIAZZI, B., ALPARONE, L., BARONTI, S. and WALD, L., 2003, Image fusion—the ARSIS concept and some successful implementation schemes. *ISPRS Journal of Photogrammetry and Remote Sensing*, **58**, pp. 4–18.
- SHETTIGARA, V.K., 1992, A generalised Component Substitution technique for spatial enhancement of multispectral images using a higher resolution data set. *Photogrammetric Engineering and Remote Sensing*, **58**, pp. 561–567.
- SMITH, A.R., 1978, Colour gamout transform pairs. *Computer Graphics*, **8**, pp. 12–18.
- STARCK, J.L. and MURTABH, R., 1994, Image restoration with noise suppression using wavelet transform. *Astronomy and Astrophysics*, **288**, pp. 342–348.
- VETTERLI, M. and KOVACEVIC, J., 1995, *Wavelets and Subband Coding* (Englewood Cliffs, NJ: Prentice-Hall).
- WALD, L., 2000, Quality of high resolution synthesized images: is there a simple criterion? *International Conference on Fusion of Earth Data, France* (Nice, France: SEE GréCA), pp. 99–105.
- WALD, L., RANCHIN, T. and MANGOLINI, M., 1997, Fusion of satellite images of different spatial resolution: assessing the quality of resulting images. *Photogrammetric Engineering and Remote Sensing*, **63**, pp. 691–699.
- WANG, Z. and BOVIK, A.C., 2002, A universal image quality index. *IEEE Signal Processing Letters*, **9**, pp. 81–84.
- YOCKY, D.A., 1995, Image merging and data fusion by means of the discrete two-dimensional wavelet transform. *Journal of the Optical Society of America*, **12**, pp. 1834–1841.
- ZHOU, J., CIVCO, D.L. and SILANDER, J.A., 1998, A wavelet transform method to merge Landsat TM and SPOT panchromatic data. *International Journal of Remote Sensing*, **19**, pp. 743–757.